

Hair Follicle–Derived Blood Vessels Vascularize Tumors in Skin and Are Inhibited by Doxorubicin

Yasuyuki Amoh,^{1,2,3} Lingna Li,¹ Meng Yang,¹ Ping Jiang,¹ Abdool R. Moossa,² Kensei Katsuoka,³ and Robert M. Hoffman^{1,2}

¹AntiCancer, Inc.; ²Department of Surgery, University of California San Diego, San Diego, California and ³Department of Dermatology, Kitasato University School of Medicine, Sagamihara, Japan

Abstract

We have recently shown that the neural-stem cell marker nestin is expressed in hair follicle stem cells and the blood vessel network interconnecting hair follicles in the skin of transgenic mice with nestin regulatory element–driven green fluorescent protein (ND-GFP). The hair follicles were shown to give rise to the nestin-expressing blood vessels in the skin. In the present study, we visualized tumor angiogenesis by dual-color fluorescence imaging in ND-GFP transgenic mice after transplantation of the murine melanoma cell line B16F10 expressing red fluorescent protein. ND-GFP was highly expressed in proliferating endothelial cells and nascent blood vessels in the growing tumor. Results of immunohistochemical staining showed that the blood vessel–specific antigen CD31 was expressed in ND-GFP–expressing nascent blood vessels. ND-GFP expression was diminished in the vessels with increased blood flow. Progressive angiogenesis during tumor growth was readily visualized during tumor growth by GFP expression. Doxorubicin inhibited the nascent tumor angiogenesis as well as tumor growth in the ND-GFP mice transplanted with B16F10-RFP. This model is useful for direct visualization of tumor angiogenesis and evaluation of angiogenic inhibitors. (Cancer Res 2005; 65(6): 2337–43)

Introduction

We report here a new model of tumor angiogenesis where we show that new blood vessels vascularizing a melanoma transplanted to the skin are derived from hair follicles in nestin-driven green fluorescent protein (ND-GFP) transgenic mice.

Recently Taylor et al. (1) reported that hair follicle bulge stem cells are potentially bipotent because they can give rise to not only cells of the hair follicle but also to epidermal cells. Other experiments (2) also have provided new evidence that the upper outer-root sheath of vibrissal (whisker) follicles of adult mice contains multipotent stem cells, which can differentiate into hair follicle matrix cells, sebaceous gland basal cells, and epidermis.

Fuchs et al. (3) engineered transgenic mice to express histone H2B linked to GFP which is controlled by a tetracycline-responsive regulatory element as well as by a keratin-5 promoter. During anagen, newly formed GFP-positive populations, derived from the bulge stem cells, formed the outer-root sheath, hair-matrix cells, hair, and inner-root sheath. Also, in response to wounding, some GFP-labeled stem cells exited the

bulge, migrated, and proliferated to repopulate the infundibulum and epidermis (3). Morris et al. (4) used the keratin-15 promoter to drive GFP in the hair-follicle bulge cells. They showed that bulge cells in adult mice generate all epithelial cell types within the intact follicle and hair during normal hair follicle cycling. After isolation, adult keratin-15-GFP-positive cells could reconstitute the cutaneous epithelium.

We previously reported that nestin, a marker for neural progenitor cells, is also selectively expressed in hair follicle stem cells (5). Follicle bulge cells, labeled with GFP driven by regulatory elements of the nestin gene (*ND-GFP*), behave as stem cells, differentiating to form much of the hair follicle each hair growth cycle.

We recently reported that many of the newly-formed nestin-expressing vessels in the skin originate from hair-follicle cells during the anagen phase. These are labeled in transgenic mice by ND-GFP. The ND-GFP vessels emerging from follicles vascularize the dermis. Their follicular origin is most evident when transplanting ND-GFP-labeled follicles to unlabeled nude mice. After transplantation of the ND-GFP hair follicles, fluorescent new blood vessels originate only from the labeled follicles. The vessels from the transplanted ND-GFP follicles responded to presumptive angiogenic signals from healing wounds. The ability to form new blood vessels must be added to the pluripotency of hair follicle stem cells (6).

In the present study, we found that nestin is a marker for proliferating endothelial cells in the nascent blood vessels vascularizing the B16F10 melanoma expressing red fluorescent protein (RFP) transplanted in the skin of ND-GFP mice.

Materials and Methods

ND-GFP Transgenic Mice. Transgenic mice carrying GFP under the control of the nestin second-intron enhancer (ND-GFP mice) were from Dr. G. Enikolopov (Cold Spring Harbor Laboratory, Cold Spring Harbor, NY; refs. 5, 6).

Visualization of Nestin Expression in Anagen Mouse Skin. Six- to 8-week-old mice with almost exclusively telogen (resting) hair follicles, were anesthetized with tribromoethanol (i.p. injection of 0.2 mL per 10 g of body weight of a 1.2% solution). The mice were depilated with a hot mixture of rosin and beeswax to induce anagen. Samples were excised from dorsal skin under anesthesia before depilation and at 48 and 72 hours after depilation, when the hair follicles were in early anagen. The skin samples were divided into three parts, one for fluorescence microscopy and the others to make frozen sections or air-dried fragments. The samples for frozen sections were embedded in tissue-freezing embedding medium (DAKO, Carpinteria, CA) and frozen at -80°C overnight. Frozen sections 5- μm thick were cut with a CM1850 cryostat (Leica, Deerfield, IL) and were air-dried.

RFP Vector Production. The RFP (*DsRed-2*) gene (BD Biosciences Clontech, Palo Alto, CA) was inserted in the retroviral-based mammalian expression vector pLNCX (BD Biosciences Clontech) to form the pLNCX DsRed-2 vector (7). Production of retrovirus resulted from transfection of pLNCX DsRed-2 into PT67 packaging cells, which produce retroviral

Requests for reprints: Robert M. Hoffman, AntiCancer, Inc., 7917 Ostrow Street, San Diego, CA 92111-3604. Phone: 858-654-2555; Fax: 858-268-4175; E-mail: all@anticancer.com.

©2005 American Association for Cancer Research.

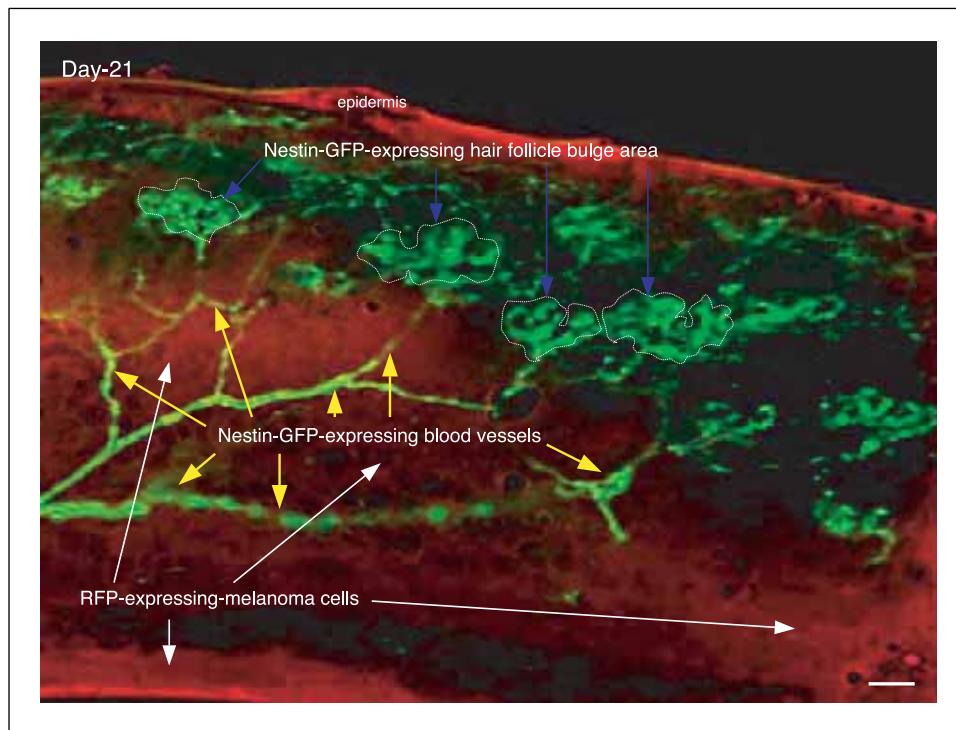


Figure 1. Hair-follicle origin of tumor angiogenic blood vessels. B16F10-RFP cells were transplanted s.c. in the ND-GFP mice. Fresh biopsied tissue was observed under fluorescence microscopy. ND-GFP vessels (yellow arrows) are visualized originating from the hair follicle bulge area and vascularizing the B16-F10-RFP tumor (white arrows). Nestin-GFP-expressing hair follicle bulge area contains the hair-follicle stem cells (blue arrows).

supernatants containing the *DSRed-2* gene. Briefly, PT67 cells were grown as monolayers in DMEM supplemented with 10% FCS (Gemini Biological Products, Calabasas, CA). Exponentially growing cells (in 10-cm dishes) were transfected with 10 μg expression vector using a LipofectAMINE Plus (Life Technologies, Grand Island, NY) protocol. Transfected cells were replated 48 hours after transfection and 100 $\mu\text{g mL}^{-1}$ G418 was added 7 hours after transfection. Two days later, the medium was changed to 200 $\mu\text{g mL}^{-1}$

G418. After 25 days of drug selection, surviving colonies were visualized under fluorescence microscopy and RFP-positive colonies were isolated. Several clones were selected and expanded into cell lines after virus titering on the 3T3 cell line.

RFP Gene Transduction of Tumor Cell Lines. For RFP gene transduction, 70% confluent rodent B16F10 melanoma cells were incubated with a 1:1 precipitated mixture of retroviral supernatants of

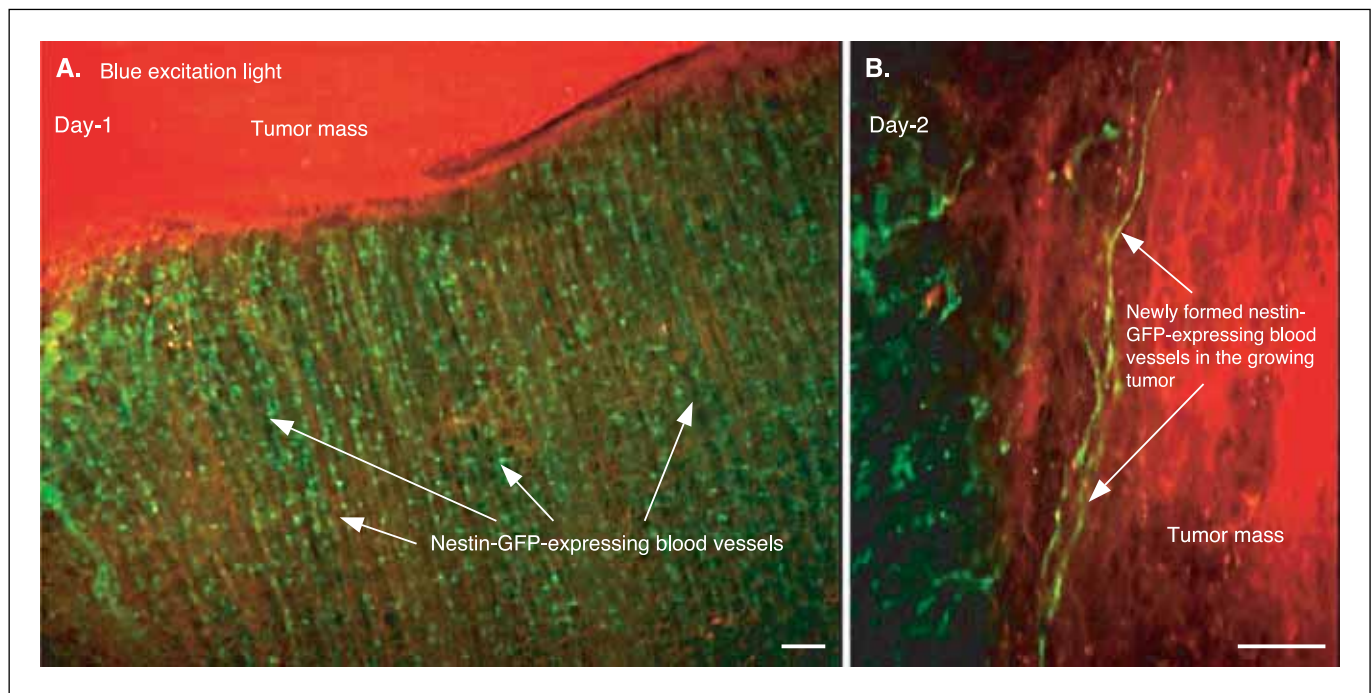


Figure 2. Early angiogenesis of tumor. A, day 1 after implantation of B16F10-RFP cells. ND-GFP vessels are visualized at the periphery of the tumor (white arrows). B, day 2 after implantation of tumor cells, ND-GFP blood vessels (white arrows) are visualized in the tumor. Bars, 100 μm .

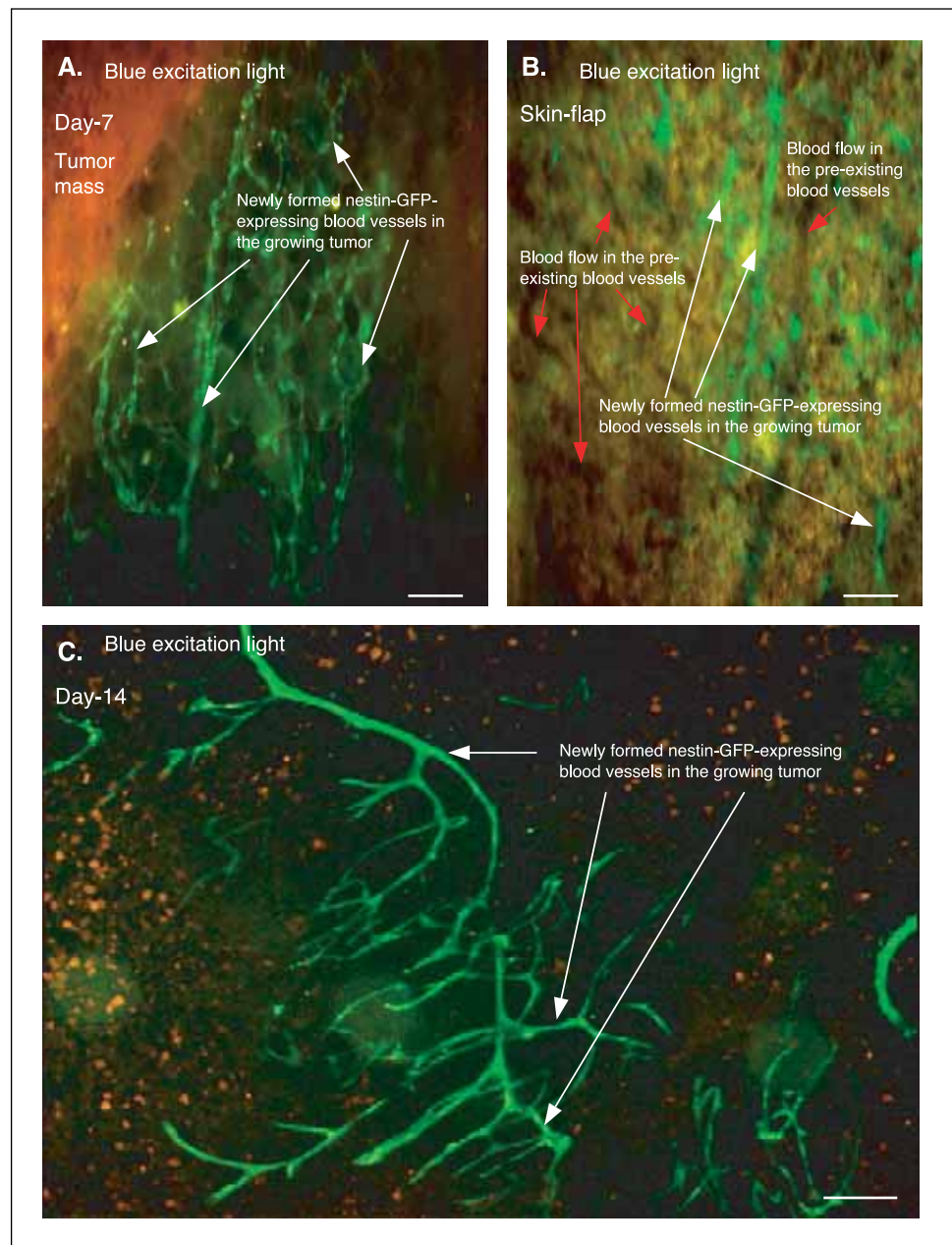


Figure 3. Intermediate-stage angiogenesis. *A*, at day 7 after implantation of tumor cells, nascent ND-GFP blood vessels (white arrows) were forming a network in the growing tumor. *B*, in a skin flap, there was apparent blood flow in the preexisting blood vessels (red arrows). However, the nascent ND-GFP vessels (white arrows) did not seem to have blood flow in the growing tumor. *C*, at day 14 after implantation of tumor cells, the ND-GFP blood vessels were forming networks. Dilatation of ND-GFP blood vessels can be seen in the growing tumor. Bars, 100 μ m.

PT67 cells and RPMI 1640 or other culture media (Life Technologies) containing 10% fetal bovine serum (Gemini Biological Products) for 72 hours. Fresh medium was replenished at this time. Tumor cells were harvested with trypsin/EDTA and subcultured at a ratio of 1:15 into selective medium, which contained 50 μ g/mL G418. To select brightly fluorescent cells, the level of G418 was increased to 800 μ g/mL in a stepwise manner. Clones expressing RFP were isolated with cloning cylinders (Bel-Art Products, Pequannock, NJ) by trypsin/EDTA and were amplified and transferred by conventional culture methods in the absence of selective agent (7).

Subcutaneous Transplantation of Tumor Cells. ND-GFP transgenic mice 6 to 8 weeks old were used. The mice were anesthetized with tribromoethanol (i.p. injection of 0.2 mL/10 g body weight of a 1.2% solution). Fifty microliters containing 2×10^6 B16F10-RFP cells were injected into the subcutis with a 1 mL 27G1/2 latex-free syringe (BD Biosciences, Bedford, MA). After the mice were anesthetized with tribromoethanol, samples of the tumor along with skin were excised at

days 1, 2, 5, 7, 14, 21, 28, and 35 after implantation of tumor cells. Samples of intestinal lymph node metastases were excised at day 28. The tissue samples were divided into two parts, one for fluorescence microscopy and the other for frozen sections. Tissue was embedded in tissue-freezing embedding medium and frozen at -80°C overnight. Frozen sections 10- μ m thick were cut with a Leica CM1850 cryostat and were air-dried. Ten mice were analyzed for each time point. Figures 1 to 7 are representative of the mice analyzed at the indicated time points. There was not significant variation between mice at each time point.

Measurement of Length of Nestin-Positive Nascent Blood Vessels and Evaluation of Antiangiogenic Effect of Doxorubicin. The mice were given daily i.p. injections of doxorubicin (5 μ g/g) or 0.9% NaCl solution (vehicle controls) at days 0, 1, and 2 after implantation of tumor cells. The mice were anesthetized with tribromoethanol, and samples of tumor mass with skin were biopsied at days 10, 14, 21, and 28 after implantation of B16F10-RFP tumor cells. At the end of experiment, the mice were euthanized. The tumors visible with the naked eye were surgically

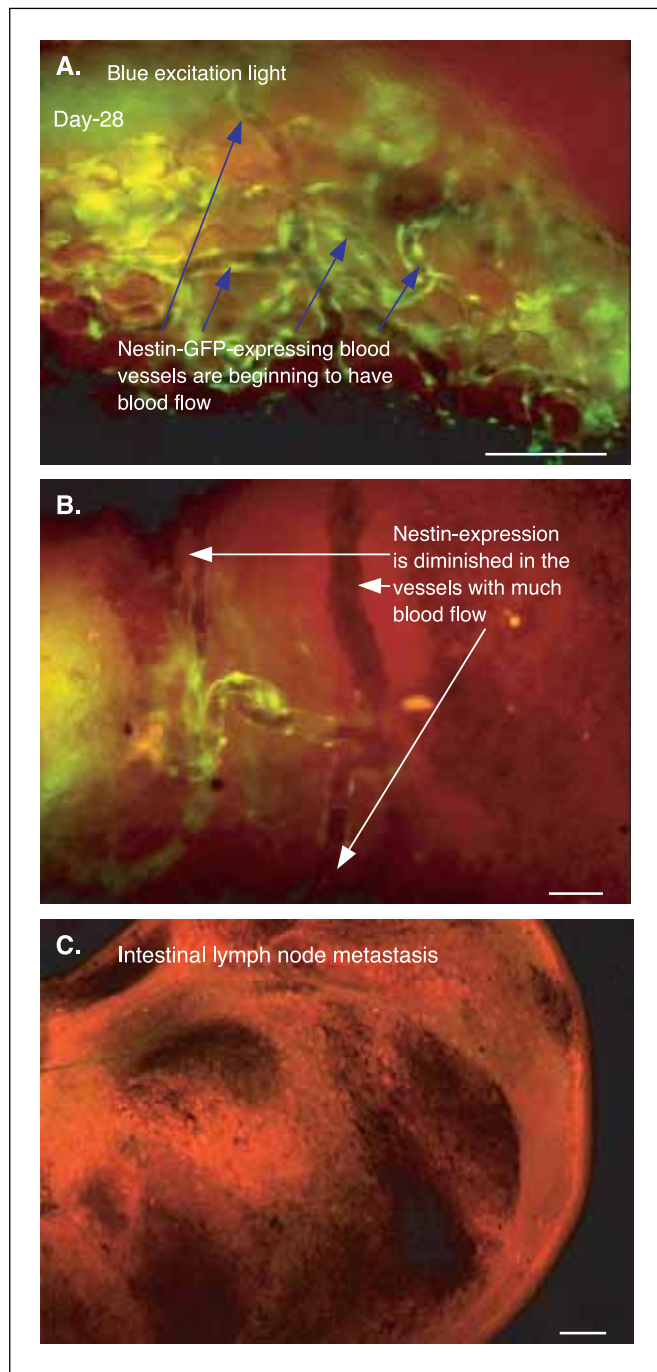


Figure 4. Late-stage angiogenesis. *A* and *B*, by day 28 after implantation of tumor cells, some ND-GFP blood vessels were beginning to have apparent blood flow (blue arrows). ND-GFP expression was diminished in the blood vessels with more blood flow (white arrows). *C*, ND-GFP blood vessels are not seen in an intestinal lymph node metastasis. Bars, 100 μm (*A*, *B*, *C*) and 10 μm (*C*).

removed. The tumors were measured in three dimensions with calipers, and tumor volume (mm^3) was calculated with the formula $V = 0.52 \times \text{length} \times \text{width} \times \text{height}$. The tumor tissue was flattened between the slide and coverslip. Angiogenesis was quantified in the tumor tissue by measuring the length of ND-GFP nascent blood vessels in all fields under fluorescence microscopy. All fields at 40 \times or 100 \times magnification were measured in order to calculate the total length of ND-GFP-positive nascent blood vessels. Moreover, the vessel density was calculated by the total length of ND-GFP nascent blood vessels divided by the tumor volume (mm^3).

Immunohistochemical Staining. Colocalization of ND-GFP fluorescence, CD31, and nestin in the frozen skin sections of the nestin-GFP transgenic mice was detected with the anti-rat immunoglobulin horseradish peroxidase detection kit (BD PharMingen, San Diego, CA; CD31) and the anti-mouse immunoglobulin horseradish peroxidase detection kit (BD PharMingen; nestin) following the manufacturer's instructions. The primary antibodies used were CD31 monoclonal antibody (1:50) and nestin monoclonal antibody (1:80). Substrate-chromogen 3,3'-diaminobenzidine staining was used for antigen detection. Anti-CD31 monoclonal antibody (CBL1337) was purchased from Chemicon (Temecula, CA). Anti-nestin monoclonal antibody (rat 401) was purchased from BD PharMingen.

Statistical Analysis. The experimental data are expressed as the mean \pm SD. Statistical analysis was done using the two-tailed Student's *t*-test.

Results and Discussion

Hair Follicle Origin of Tumor Angiogenesis

We had previously shown that hair follicles in the skin gave rise to blood vessels (6). In the present study, we show that the vessels vascularizing the transplanted B16F10-RFP melanoma cells originate from the hair follicles (Fig. 1). The tumor angiogenic blood vessels seem to be originating from the bulge area of the hair follicles which strongly express nestin and contain the hair follicle stem cells (5).

Time Course of Tumor Angiogenesis Visualized by ND-GFP Blood Vessels

Early Tumor Angiogenesis Visualized by ND-GFP. At day 1 after implantation, RFP-positive tumor cells were visualized growing in the subcutis including the muscularis. At this time, ND-GFP-expressing blood vessels of the subcutis could be seen at the periphery of the RFP-positive tumor cells. By day 2, ND-GFP-expressing blood vessels were growing into the tumor. By day 5, numerous ND-GFP-expressing blood vessels were visualized in the growing tumor (Fig. 2).

Intermediate Tumor Angiogenesis Visualized by ND-GFP. By day 7 after implantation of tumor cells, ND-GFP-expressing blood vessels were forming a network in the growing tumor (Fig. 3A). Blood flow in the preexisting blood vessels could be visualized via skin flaps. However, the ND-GFP-expressing vessels did not seem to have blood flow in the growing tumor (Fig. 3B). By day 14, ND-GFP-expressing blood vessels with vessel dilation could be seen in the growing tumor (Fig. 3C). Vessel dilation occurs before blood flow can occur in a developing vessel.

Late-Stage Angiogenesis Visualized by ND-GFP. By day 28 after implantation of tumor cells, some ND-GFP-expressing blood vessels were beginning to have apparent blood flow (Fig. 4A). However, ND-GFP expression was extinguished in the blood vessels with apparent blood flow (Fig. 4B). By day 35 after implantation of tumor cells, large vessels had apparent blood flow in the growing tumor. ND-GFP expression was diminished in the blood vessels with significant blood flow. ND-GFP expression was maintained in the peripheral area of the tumor. In contrast to the skin, ND-GFP-expressing blood vessels were not visualized in the intestinal lymph node metastasis of the B16F10-RFP melanoma (Fig. 4C).

Immunohistochemical staining showed that CD31 and nestin were colocalized in the blood vessels in the growing tumor. A frozen section showing the ND-GFP blood vessels and RFP-expressing B16F10 melanoma was compared with a sister section stained for CD31 demonstrating colocalization of ND-GFP and CD31 (Fig. 5).

Visualization of Intravasated Tumor Cells

By day 7, RFP-expressing B16F10 melanoma cells could be seen inside the ND-GFP blood vessels (Fig. 6). These results suggest that the ND-GFP blood vessels can be used by the tumor cells for hematogenous metastasis. The dual-color model shows that hematogenous metastasis is readily imaged.

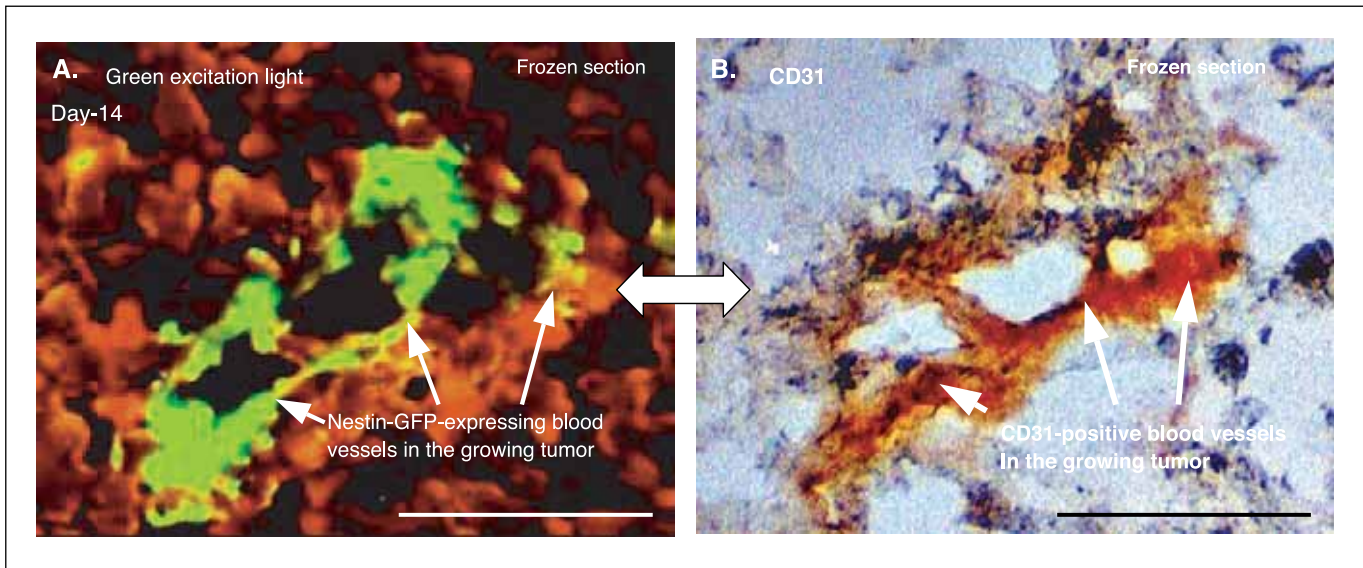


Figure 5. Immunohistochemical staining of CD31. *A*, ND-GFP (white arrows) is visualized in blood vessels in the B16F10-RFP tumor in a frozen section. *B*, immunohistochemical staining in a sister frozen section shows CD31 (black arrows) colocalizing with ND-GFP blood vessels in the growing tumor. Bars, 100 μ m.

Effects of Doxorubicin on Tumor Growth and Angiogenesis

Mice were given daily i.p. injections of 5 μ g/g of doxorubicin at days 0, 1, and 2 after implantation of the B16F10-RFP melanoma cells. This protocol was used in order to minimize doxorubicin toxicity. At day 10 after implantation, only the marginal area of the tumor had ND-GFP-expressing blood vessels in the treated animals. ND-GFP-expressing blood vessels were not observed in the central area of the tumor. The number of ND-GFP-expressing blood vessels was much less in the doxorubicin-

treated animals than in NaCl-injected control mice (Fig. 7*A*). Tumor volume was determined on days 10, 14, and 21 after implantation of tumor cells. Treatment with doxorubicin significantly decreased tumor volume as well as nascent blood vessel formation. By day 10 after implantation of tumor cells, treatment with doxorubicin significantly decreased the mean nascent blood vessel length per tumor volume (Fig. 7; * $P < 0.05$ versus NaCl solution-injected mice). These results show the utility of the dual-color ND-GFP mouse-RFP-tumor model to visualize and quantitate angiogenesis and to screen for angiogenesis

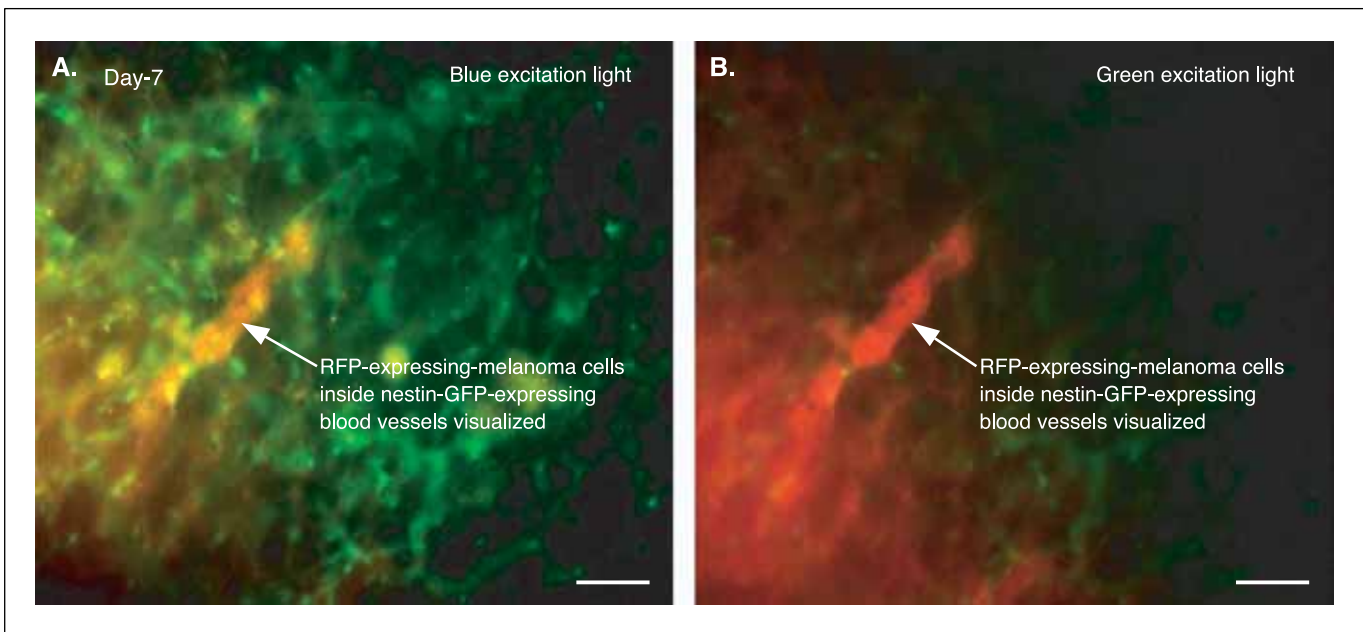


Figure 6. Visualization of intravasated tumor cells. B16F10-RFP tumor cells are seen inside ND-GFP blood vessels. Tumor tissue was biopsied from ND-GFP animals transplanted with B16F10-RFP cells and visualized as fresh tissue under fluorescence microscopy. *A*, under blue excitation light, the RFP tumor cells in the GFP vessels appear orange. The vessels without tumor cells have green fluorescence. *B*, under green excitation light, the tumor cells in the vessels appear red.

inhibitors. Brown et al. (8) showed that multiphoton laser-scanning microscopy can provide high three-dimensional resolution of vascular endothelial growth factor-driven GFP gene expression in fibroblasts in tumors implanted in a window chamber in the dorsal skin of mice. In our study, the ND-GFP transgenic mice enable the visualization of the nascent blood

vessels themselves in the tumor as they originate from the hair follicles.

Angiogenesis plays an important role in understanding tissue maintenance, wound repair, and the growth of tumors and necrosis (9). Identifying the source of the cells for new blood vessels has become increasingly important both scientifically and

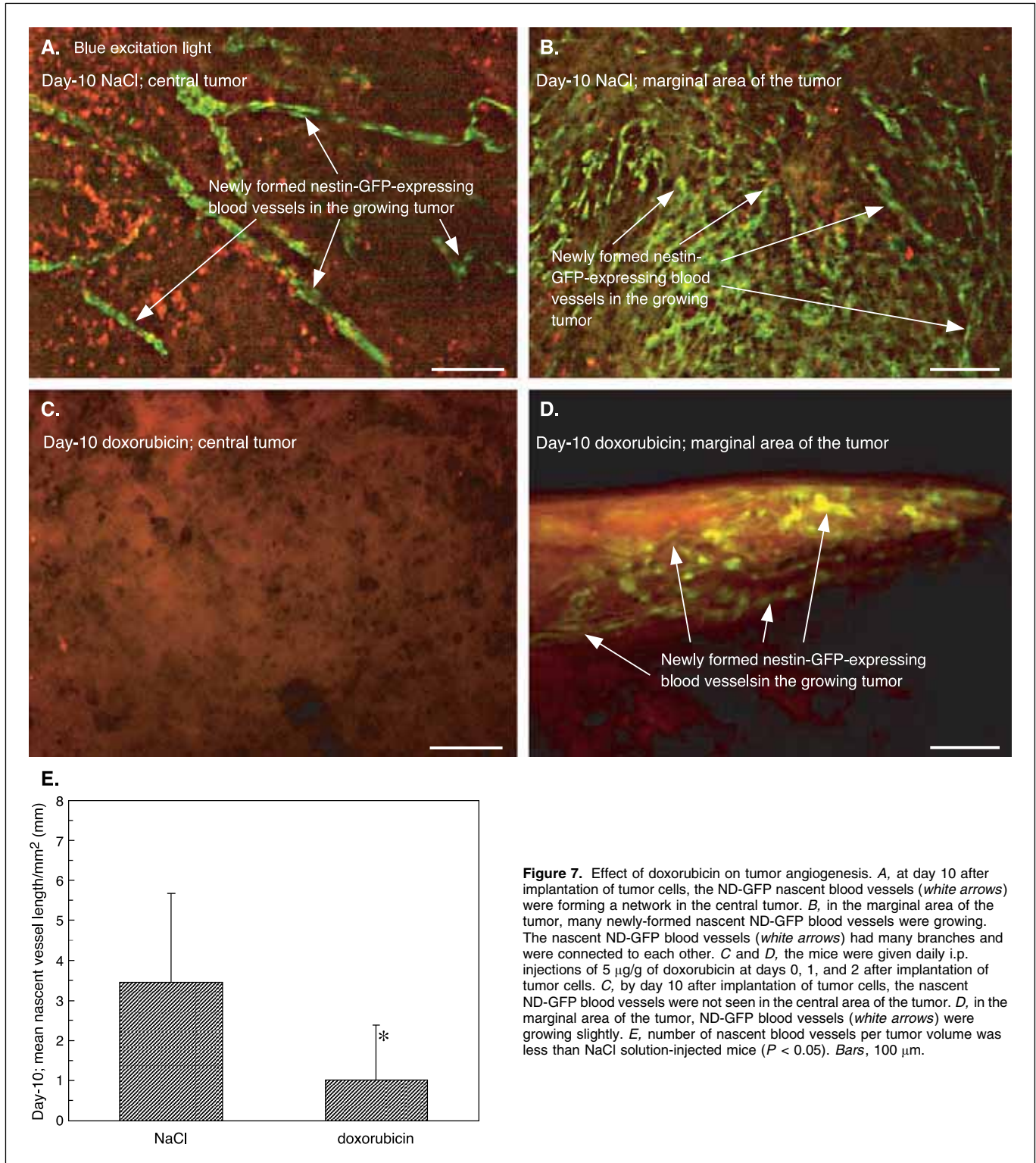


Figure 7. Effect of doxorubicin on tumor angiogenesis. *A*, at day 10 after implantation of tumor cells, the ND-GFP nascent blood vessels (*white arrows*) were forming a network in the central tumor. *B*, in the marginal area of the tumor, many newly-formed nascent ND-GFP blood vessels were growing. The nascent ND-GFP blood vessels (*white arrows*) had many branches and were connected to each other. *C* and *D*, the mice were given daily i.p. injections of 5 μg/g of doxorubicin at days 0, 1, and 2 after implantation of tumor cells. *C*, by day 10 after implantation of tumor cells, the nascent ND-GFP blood vessels were not seen in the central area of the tumor. *D*, in the marginal area of the tumor, ND-GFP blood vessels (*white arrows*) were growing slightly. *E*, number of nascent blood vessels per tumor volume was less than NaCl solution-injected mice ($P < 0.05$). Bars, 100 μm.

for therapeutic design. There have been numerous recent reports of endothelial cells arising from bone marrow-derived stem cells (10). There is also evidence that endothelial stem cells can be derived from adipose tissue (6). However, these previously identified sources of endothelial stem cells may not be able to supply blood vessels in the skin because of skin's unique structure. The results presented here indicate that hair follicle stem cells supply endothelial cells that can form blood vessels in the skin and in tumors growing in the skin. Recently, Toma et al. (11) reported that multipotent adult stem cells isolated from mammalian dermis, termed skin-derived precursors, can proliferate and differentiate in culture to produce neurons, glia, smooth muscle

cells, and adipocytes. The pluripotency of the hair follicle stem cells suggested by the present study and our previous results (5, 6) suggest that many of the stem cells isolated by Toma et al. may have originated in the hair follicle.

Acknowledgments

Received 11/1/2004; revised 12/14/2004; accepted 1/7/2005.

Grant support: U.S. National Cancer Institute grants CA099258, CA103563, and CA101600.

The costs of publication of this article were defrayed in part by the payment of page charges. This article must therefore be hereby marked *advertisement* in accordance with 18 U.S.C. Section 1734 solely to indicate this fact.

References

1. Taylor G, Lehrer MS, Jensen PJ, Sun T-T, Lavker RM. Involvement of follicular stem cells in forming not only the follicle but also the epidermis. *Cell* 2000;102:451-61.
2. Oshima H, Rochat A, Kedzia C, Kobayashi K, Barrandon Y. Morphogenesis and renewal of hair follicles from adult multipotent stem cells. *Cell* 2001;104:233-45.
3. Tumber T, Guasch G, Greco V, et al. Defining the epithelial stem cell niche in skin. *Science* 2004;303:359-63.
4. Morris RJ, Liu Y, Marles L, et al. Capturing and profiling adult hair follicle stem cells. *Nat Biotechnol* 2004;22:411-7.
5. Li L, Mignone J, Yang M, et al. Nestin expression in hair follicle sheath progenitor cells. *Proc Natl Acad Sci U S A* 2003;100:9958-61.
6. Amoh Y, Li L, Yang M, et al. Nascent blood vessels in the skin arise from nestin-expressing hair follicle cells. *Proc Natl Acad Sci U S A* 2004;101:13291-5.
7. Yang M, Li L, Jiang P, Moossa AR, Penman S, Hoffman RM. Dual-color fluorescence imaging distinguishes tumor cells from induced host angiogenic vessels and stromal cells. *Proc Natl Acad Sci U S A* 2003;100:14259-62.
8. Brown EB, Campbell RB, Tsuzuki Y, et al. *In vivo* measurement of gene expression, angiogenesis, and physiological function in tumors using multiphoton laser scanning microscopy. *Nat Med* 2001;7:864-8.
9. Yano K, Brown LF, Detmar M. Control of hair growth and follicle size by VEGF-mediated angiogenesis. *J Clin Invest* 2001;107:409-17.
10. Mecklenburg L, Tobin DJ, Muller-Rover S, et al. Active hair growth (anagen) is associated with angiogenesis. *J Invest Dermatol* 2000;114:909-16.
11. Toma JG, Akhavan M, Fernandes JL, et al. Isolation of multipotent adult stem cells from the dermis of mammalian skin. *Nat Cell Biol* 2001;3:778-84.